Star Formation Newsletter #343 1-7

大橋聡史（理研）

- 1. Multi-scale Dust Polarization and Spiral-like Stokes-I Residual in the Class I Protostellar System TMC-1A
- 2. PV Cep and V350 Cep: stars on the way between FUors AND EXors
- 3. GIARPS High-resolution Observations of T Tauri stars (GHOsT). III. A pilot study of stellar and accretion properties
- 4. Evolution of the angular momentum during gravitational fragmentation of molecular clouds
- 5. Classification of Filament Formation Mechanisms in Magnetized Molecular Clouds
- 6. Detection of coherent low-frequency radio bursts from weak-line TTauri stars
- 7. The Transition from Diffuse Molecular Gas to Molecular Cloud Material in Taurus

Multi-scale Dust Polarization and Spiral-like Stokes-I Residual in the Class I Protostellar System TMC-1A

Yusuke Aso, Woojin Kwon, Naomi Hirano, Tao-Chung Ching, Shih-Ping Lai, Zhi-Yun Li, Ramprasad Rao

SMAとALMAでTMC1A周りのダスト偏光観測

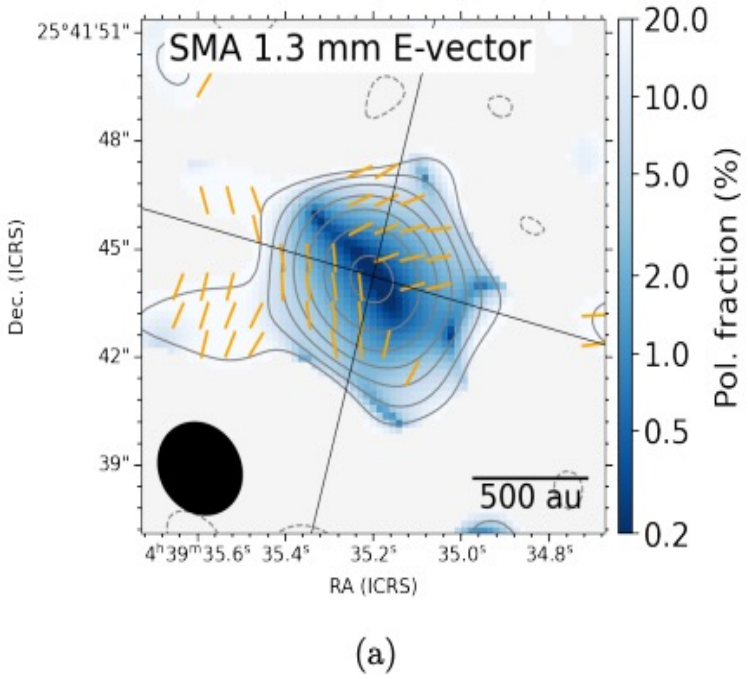

(a)

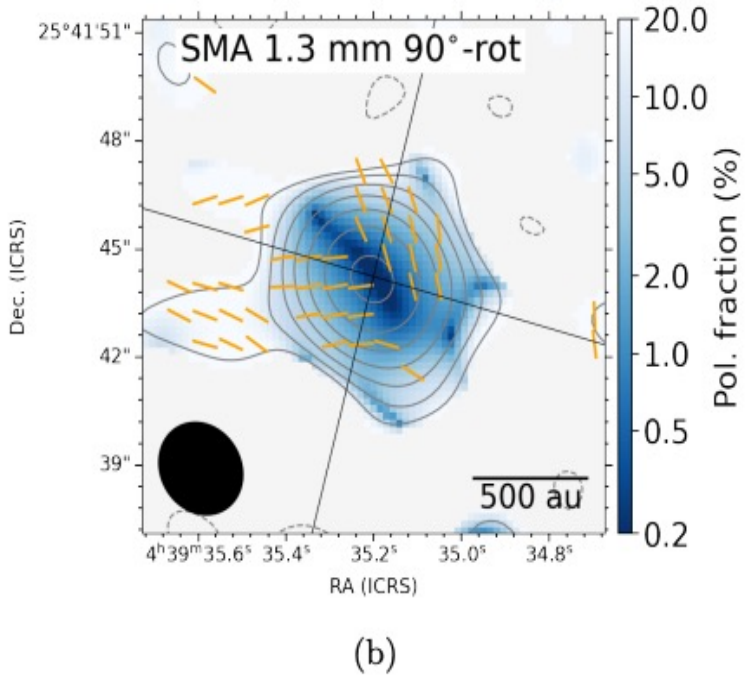

(b)

SMAの観測では磁場を観測
→チャンドラセカールフェルミ法で磁場強度を推定 ~ 1-5 mG

過去の研究で中心星へのinfall 速度がfree fallの0.3倍であり、磁場によって速度が遅くなっている。（磁場強度3mG)

遅いインフォールと一致

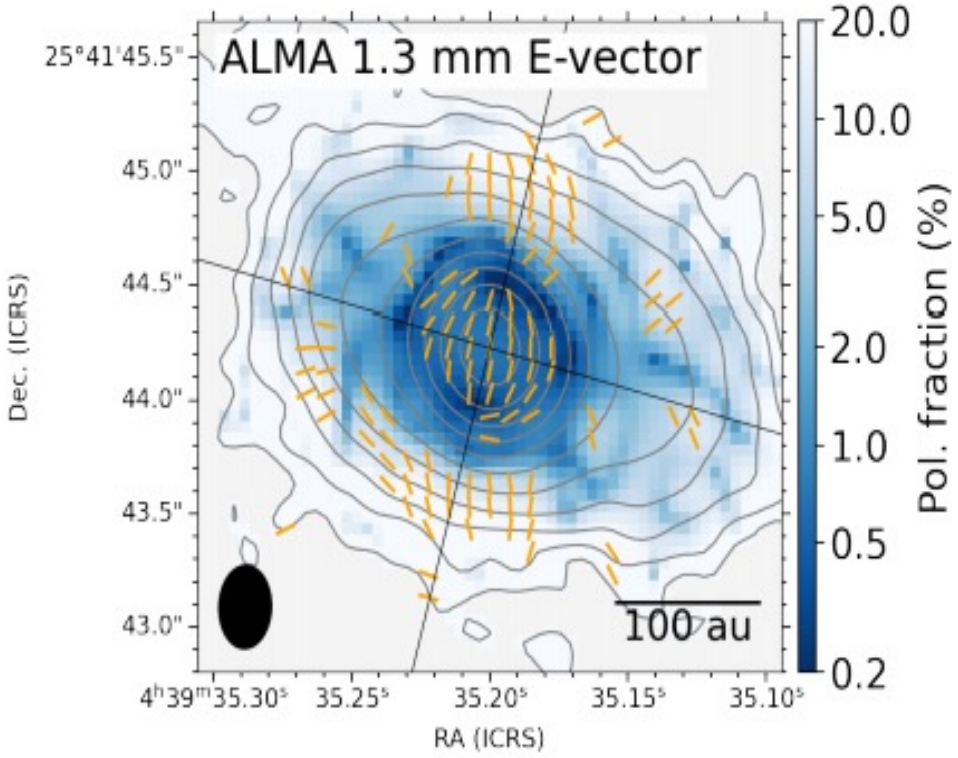

(a)

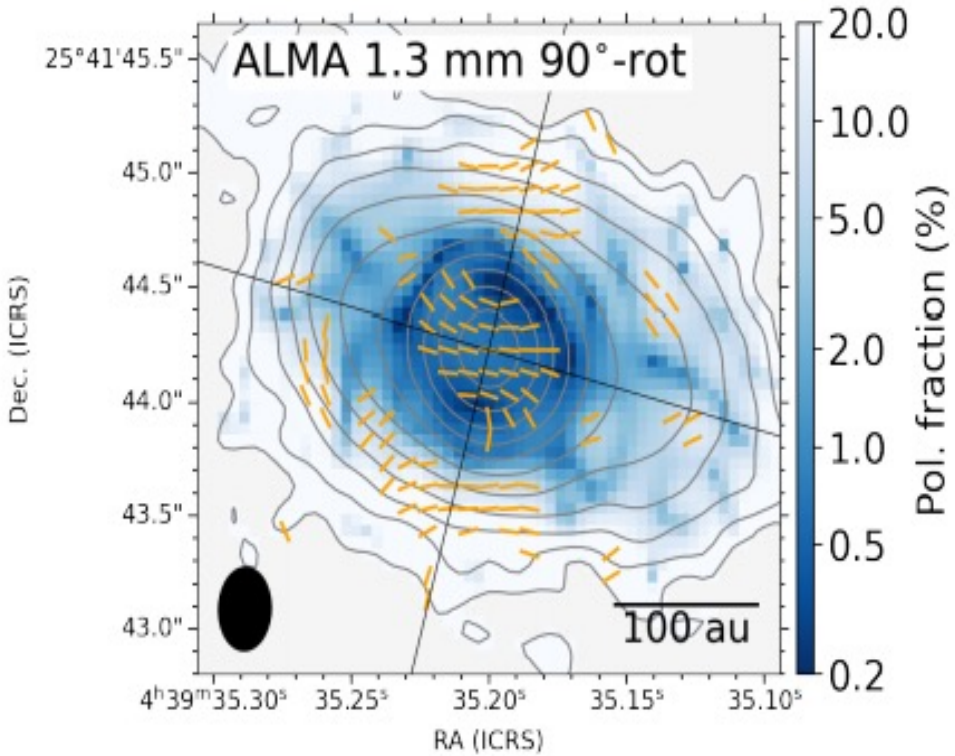

(b)

中心領域では偏光ベクトルが円盤の短軸と一緒→自己散乱(~ 100ミクロン)による

100 auスケールではradial 方向に沿った偏光ベクトル
→磁場に整列している可能性がある(mechanical alignmentはless likely)

偏光の高感度の観測からStokes Iの強度分布も調べた。結果、非軸対象な構造＋リングを発見

Residual mapにspiral構図

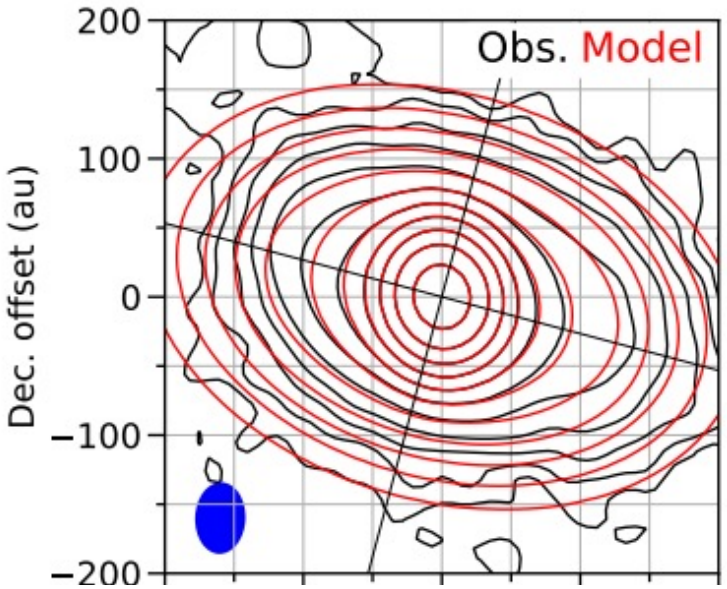

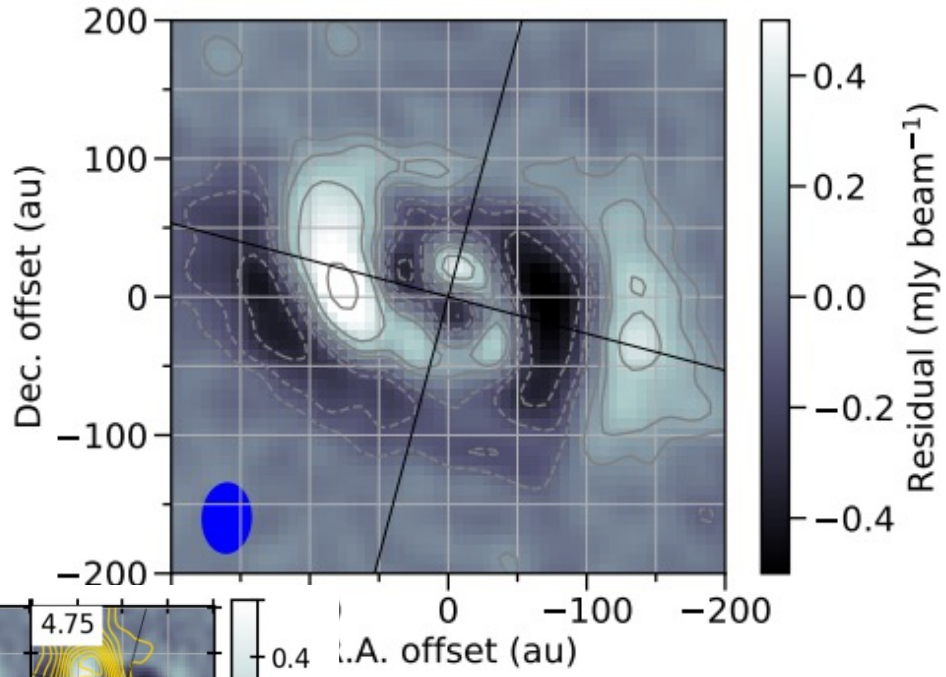

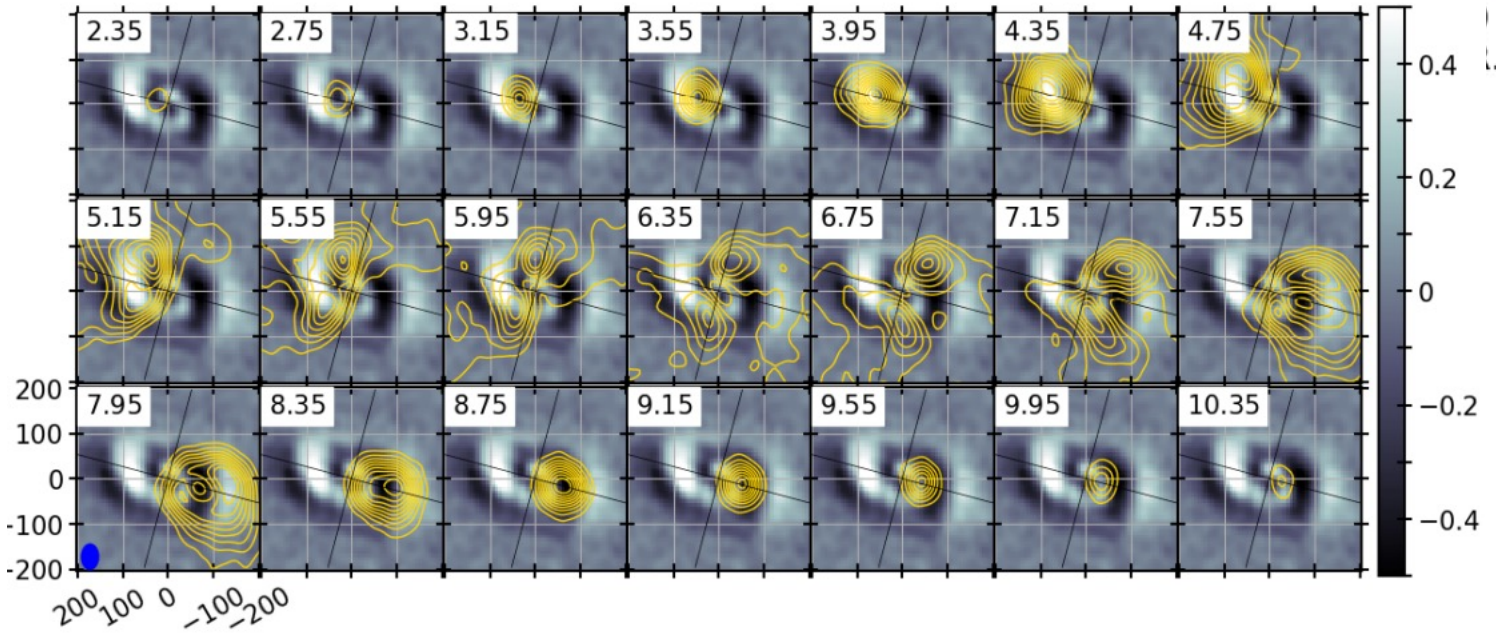

C18Oのチャンネルマップと構造が一致
→ spiralに円盤降着？

50 auのリングはgrowth front?

Evolution of the angular momentum during gravitational fragmentation of molecular clouds

G. Arroyo-Chávez, E. Vázquez-Semadeni

分子雲や分子雲コアで観測されている比角運動量vsサイズの関係をglobal hierarchical collapseによるシミュレーション

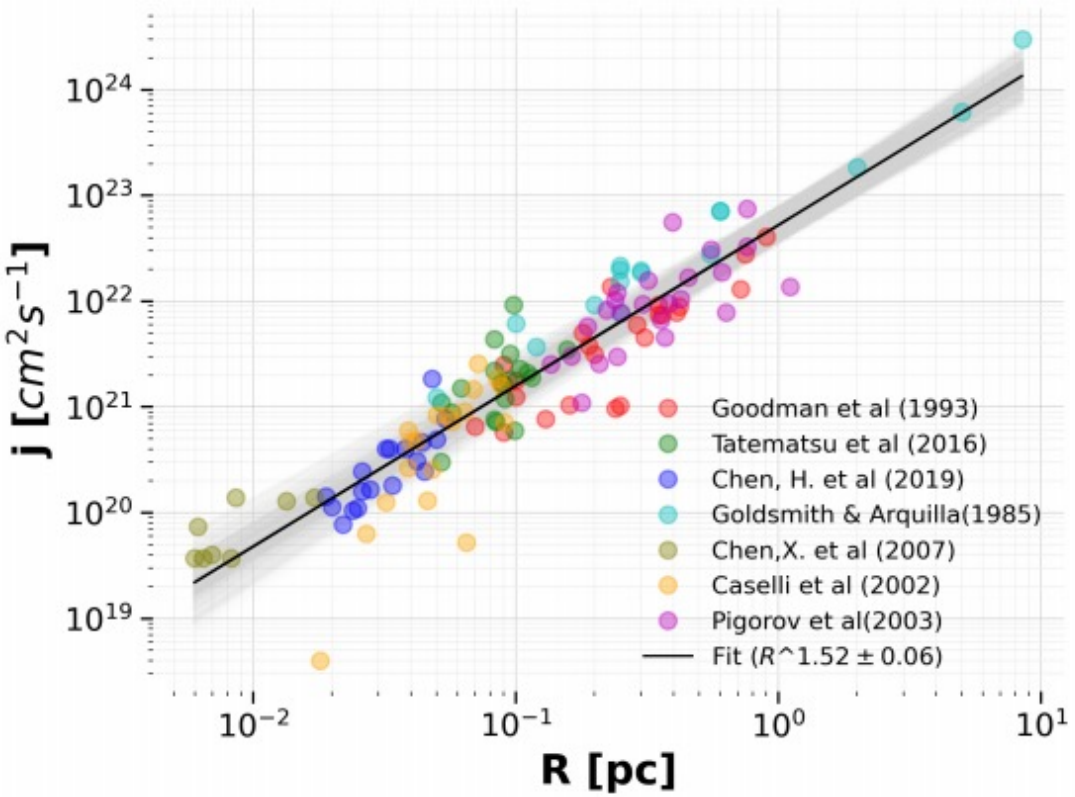

$$\int_V \boldsymbol{r} \times \frac{\partial(\rho \boldsymbol{u})}{\partial t} dV = -\int_V \boldsymbol{r} \times \nabla \cdot (\rho \boldsymbol{u}\boldsymbol{u}) dV - \int_V \boldsymbol{r} \times \nabla P dV - \int_V \boldsymbol{r} \times \rho \nabla \phi dV + \int_V \boldsymbol{r} \times \mu(\nabla^2 \boldsymbol{u} + \nabla\nabla \cdot \boldsymbol{u}\boldsymbol{u}) dV + \int_V \boldsymbol{r} \times \frac{1}{4\pi}(\nabla \times \boldsymbol{B}) \times \boldsymbol{B} dV, \quad (1)$$

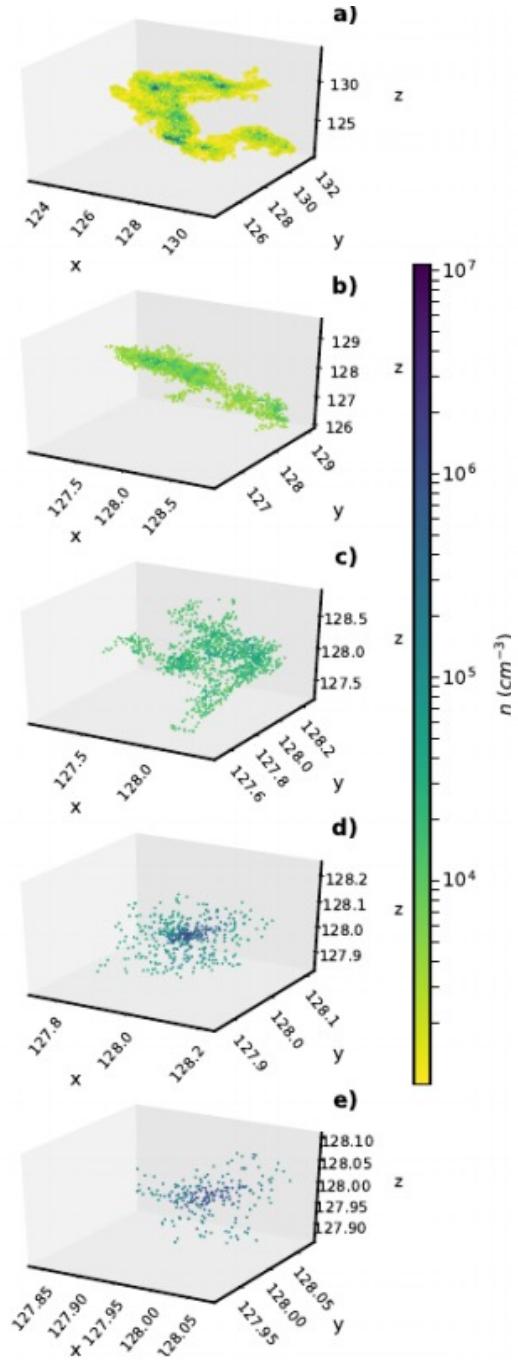

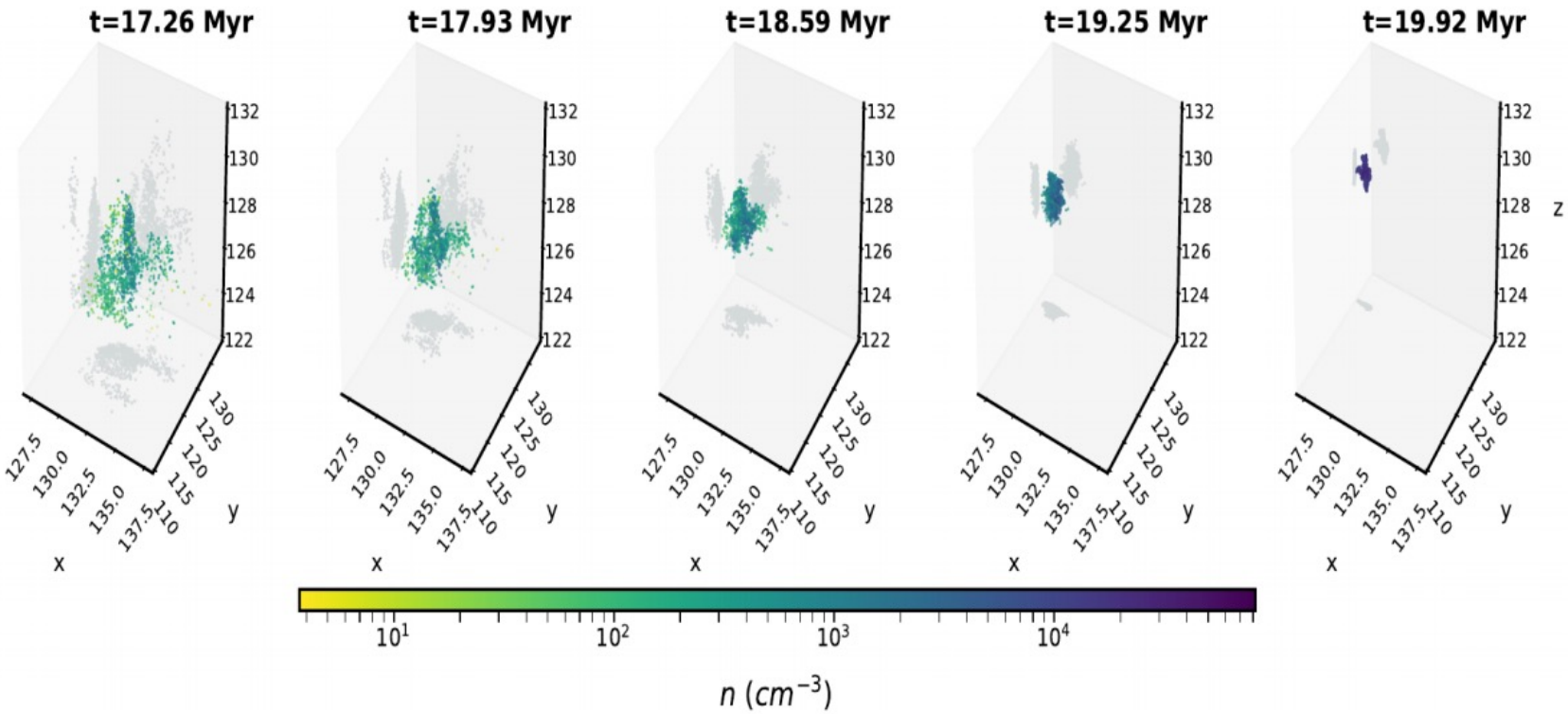

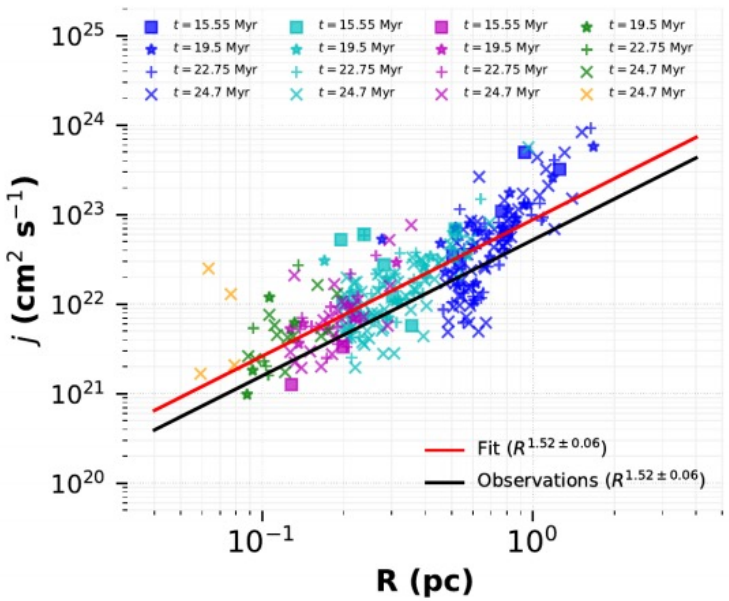

分子雲コアのように小さなスケールで高密度な領域は
角運動量をdiffuse gasに渡すことで形成する
(accretion diskと考えは同じ)

時間進化

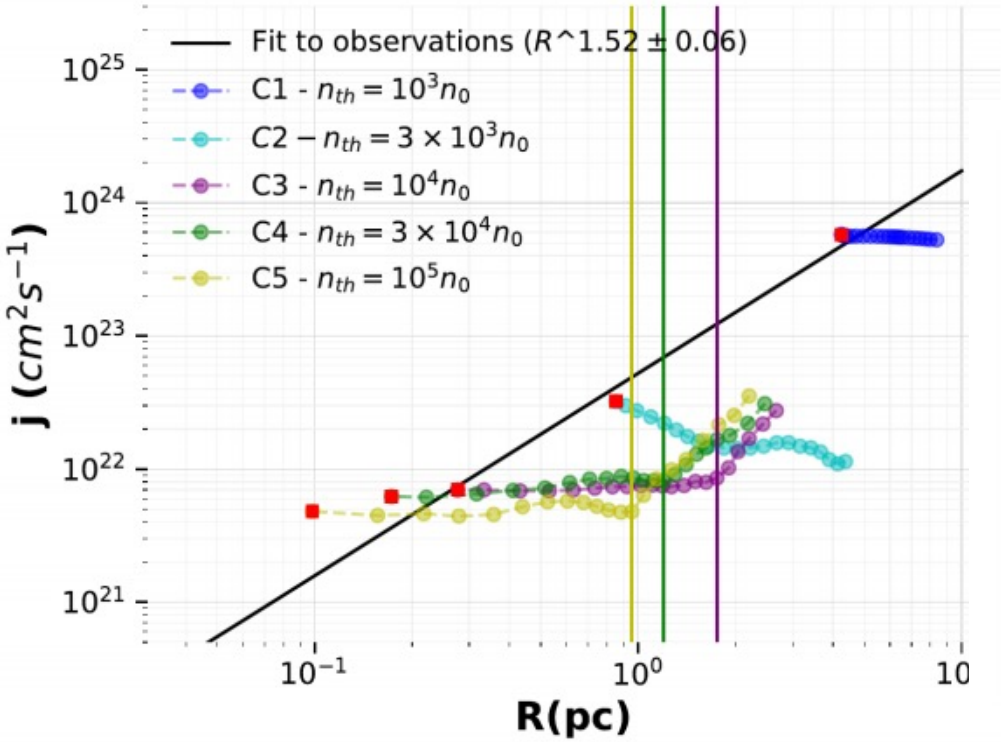
Fit to observations (R^1.52 ± 0.06)
C1 - $n_{th} = 10^3 n_0$
C2 – $n_{th} = 3 \times 10^3 n_0$
C3 - $n_{th} = 10^4 n_0$
C4 - $n_{th} = 3 \times 10^4 n_0$
C5 - $n_{th} = 10^5 n_0$
10^{25}
10^{24}
10^{23}
10^{22}
10^{21}
j ($cm^2 s^{-1}$)
10^{-1}
10^0
10
R(pc)

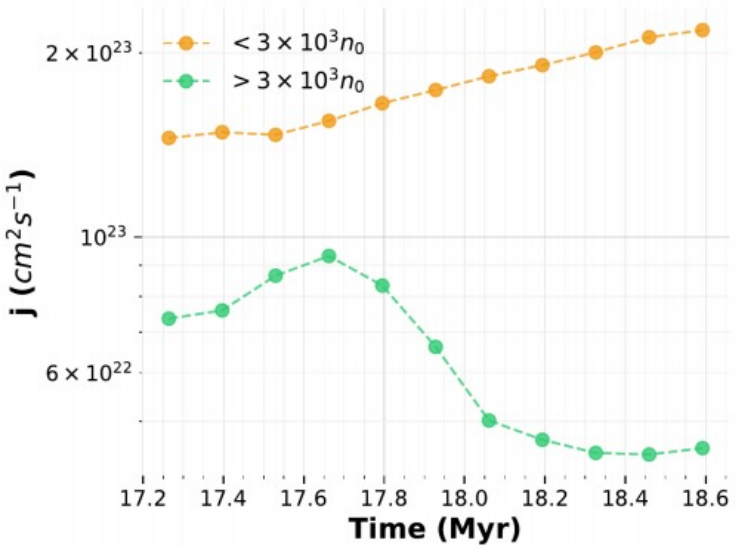
$< 3 \times 10^3 n_0$
$> 3 \times 10^3 n_0$
2×10^{23}
10^{23}
6×10^{22}
j ($cm^2 s^{-1}$)
17.2
17.4
17.6
17.8
18.0
18.2
18.4
18.6
Time (Myr)

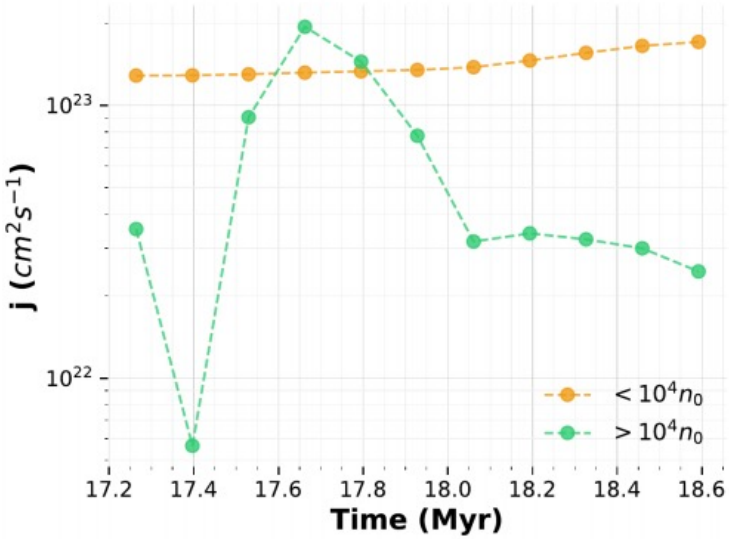
10^{23}
10^{22}
j ($cm^2 s^{-1}$)
$< 10^4 n_0$
$> 10^4 n_0$
17.2
17.4
17.6
17.8
18.0
18.2
18.4
18.6
Time (Myr)

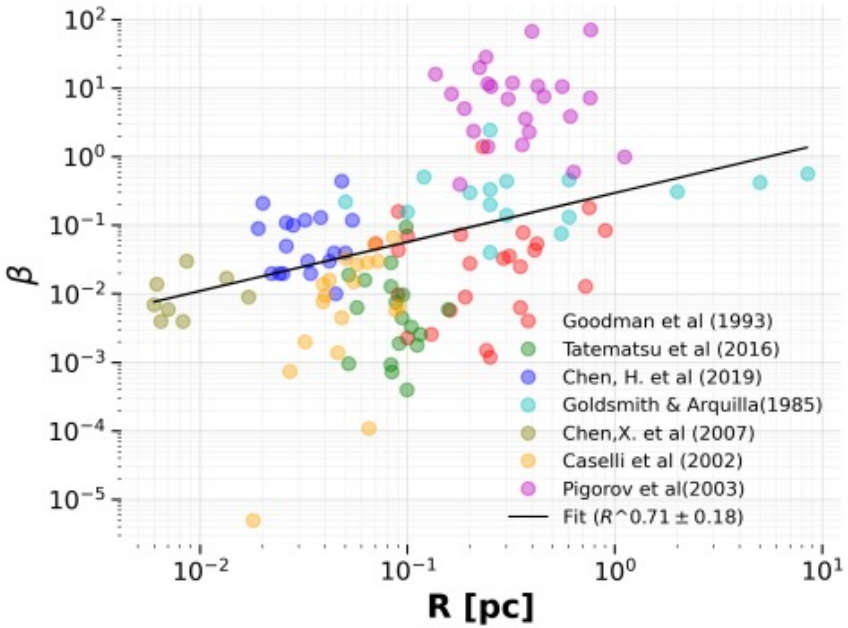

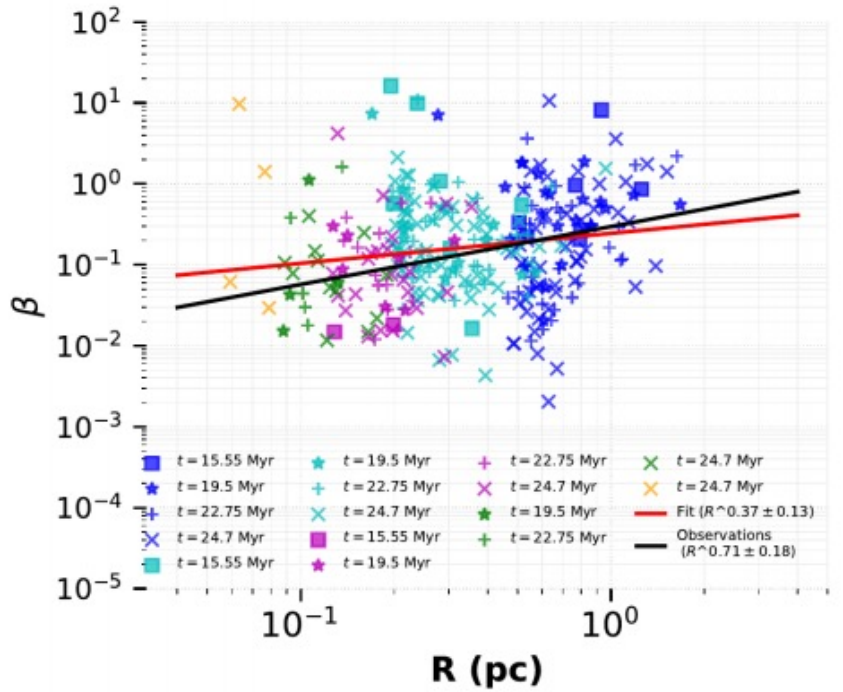

回転エネルギーと重力エネルギーの割合(β)はほとんど一定

$$\beta \equiv \frac{e_{\rm r}}{e_{\rm g}} \approx \frac{1/2\, j\omega}{\pi G R \Sigma}. \tag{14}$$

Under the assumption that $\beta \approx$ cst., we can then solve for ω as

$$\omega \approx \frac{2\pi\beta G R \Sigma}{j}. \tag{15}$$

On the other hand, the SAM is $j = I\omega/M \approx R^2\omega$. Substituting eq. (15) in this expression for j, we finally get

$$j \approx (2\pi\beta G\Sigma)^{1/2} R^{3/2}, \tag{16}$$

PV Cep and V350 Cep: stars on the way between FUors AND EXors

H. R. Andreasyan, T. Yu. Magakian, T. A. Movsessian, A. V. Moiseev

Based on new observations during 2015-2020 and published data, the unusual eruptive variables PV Cep and V350 Cep are examined. It is shown that PV Cep underwent a regular outburst followed by a drop in brightness that lasted overall from 2011 to 2019 and is still in a deep minimum. The outburst was accompanied by substantial changes in the intensity and profiles of a number of lines, including Ha, [SII], and [OI]. The forbidden lines generally have negative radial velocities and can be divided into four components, with variable velocities and relative intensities. V350 Cep essentially is at a maximum brightness level over the entire time and its spectrum is practically unaltered. The available data suggest that the pronounced P Cyg profile of the Ha line in the spectrum of V350 Cep appeared several years after the luminosity rise, in 1986. The luminosities of the stars in the current state are estimated to be 20 L(sun) and 3.3 L(sun), respectively. It is concluded that both stars may represent a so-called intermediate objects between the FUor and EXor classes.

GIARPS High-resolution Observations of T Tauri stars (GHOsT). III. A pilot study of stellar and accretion properties

J. M. Alcalá, M. Gangi, K. Biazzo, S. Antoniucci, A. Frasca, T. Giannini, U. Munari, B. Nisini, A. Harutyunyan, C. F. Manara, F. Vitali

The mass-accretion rate, Macc, is a crucial parameter for the study of the evolution of accretion disks around young low-mass stellar objects (YSOs) and for planet formation studies. The Taurus star forming region (SFR) is rich in pre-main sequence (PMS) stars, most of them of the T Tauri class. A variety of methodologies have been used in the past to measure mass accretion in samples of YSOs in Taurus, but despite being a general benchmark for star formation studies, a comprehensive and systematic analysis of the Taurus T Tauri population, where the stellar and accretion properties are derived homogeneously and simultaneously, is still missing. As part of the GIARPS High-resolution Observations of T Tauri stars (GHOsT) project, here we present a pilot study of the stellar and accretion properties of seven YSOs in Taurus using the spectrograph GIARPS at the Telescopio Nazionale Galileo (TNG). Contemporaneous low-resolution spectroscopic and photometric ancillary observations allow us to perform an accurate flux calibration of the high-resolution spectra. The simultaneity of the high-resolution, wide-band spectroscopic observations, from the optical to the near-infrared (NIR), the veiling measurements in such wide spectral range, and many well-calibrated emission line diagnostics allows us to derive the stellar and accretion properties of the seven YSOs in a homogeneous and self-consistent way. The procedures and methodologies presented here will be adopted in future works for the analysis of the complete GHOsT data set. We discuss the accretion properties of the seven YSOs in comparison with the 90% complete sample of YSOs in the Lupus SFR and investigate possibilities for the origin of the continuum excess emission in the NIR.

Classification of Filament Formation Mechanisms in Magnetized Molecular Clouds

Daisei Abe, Tsuyoshi Inoue, Shu-ichiro Inutsuka, Tomoaki Matsumoto

Recent observations of molecular clouds show that dense filaments are the sites of present-day star formation. Thus, it is necessary to understand the filament formation process because these filaments provide the initial condition for star formation. Theoretical research suggests that shock waves in molecular clouds trigger filament formation. Since several different mechanisms have been proposed for filament formation, the formation mechanism of the observed star-forming filaments requires clarification. In the present study, we perform a series of isothermal magnetohydrodynamics simulations of filament formation. We focus on the influences of shock velocity and turbulence on the formation mechanism and identified three different mechanisms for the filament formation. The results indicate that when the shock is fast, at shock velocity $v_{sh} = 7$ km/s, the gas flows driven by the curved shock wave create filaments irrespective of the presence of turbulence and self-gravity. However, at a slow shock velocity $v_{sh} = 2.5$ km/s, the compressive flow component involved in the initial turbulence induces filament formation. When both the shock velocities and turbulence are low, the self-gravity in the shock-compressed sheet becomes important for filament formation. Moreover, we analyzed the line-mass distribution of the filaments and showed that strong shock waves can naturally create high-line-mass filaments such as those observed in the massive star-forming regions in a short time. We conclude that the dominant filament formation mode changes with the velocity of the shock wave triggering the filament formation.

Detection of coherent low-frequency radio bursts from weak-line TTauri stars

A. Feeney-Johansson, S. J. D. Purser, T. P. Ray, A. A. Vidotto, J. Eislöffel, J. R. Callingham, T. W. Shimwell, H. K. Vedantham, G. Hallinan, C. Tasse

In recent years, thanks to new facilities such as LOFAR capable of sensitive observations, much work has been done on the detection of stellar radio emission at low frequencies. Such emission has commonly been shown to be coherent emission, generally attributed to electron-cyclotron maser emission, and has usually been detected from main-sequence M dwarfs. Here we report the first detection of coherent emission at low frequencies from T Tauri stars, which are known to be associated with high levels of stellar activity. Using LOFAR, we have detected several bright radio bursts at 150 MHz from two weak-line T Tauri stars: KPNO-Tau 14 and LkCa 4. All of the bursts have high brightness temperatures ($10^{13} - 10^{14}$ K) and high circular polarization fractions (60 - 90 %), indicating that they must be due to a coherent emission mechanism. This could be either plasma emission or electron-cyclotron maser (ECM) emission. Due to the exceptionally high brightness temperatures seen in at least one of the bursts ($\geq 10^{14}$ K), and the high circular polarization levels, it seems unlikely that plasma emission could be the source and so ECM is favoured as the most likely emission mechanism. Assuming this is the case, the required magnetic field in the emission regions would be 40 - 70 G. We determine that the most likely method of generating ECM emission is plasma co-rotation breakdown in the stellar magnetosphere. There remains the possibility, however, it could be due to an interaction with an orbiting exoplanet.

The Transition from Diffuse Molecular Gas to Molecular Cloud Material in Taurus

S. R. Federman, Johnathan S. Rice, A. M. Ritchey, Hwihyun Kim, John H. Lacy, Paul F. Goldsmith, Nicolas Flagey, Gregory N. Mace, David L. Lambert

We study four lines of sight that probe the transition from diffuse molecular gas to molecular cloud material in Taurus. Measurements of atomic and molecular absorption are used to infer the distribution of species and the physical conditions toward stars behind the Taurus Molecular Cloud (TMC). New high-resolution spectra at visible and near infrared wavelengths of interstellar Ca II, Ca I, K I, CH, CH^+, C2, CN, and CO toward HD28975 and HD29647 are combined with data at visible wavelengths and published CO results from ultraviolet measurements for HD27778 and HD30122. Gas densities and temperatures are inferred from C2, CN, and CO excitation and CN chemistry. Our results for HD29647 are noteworthy because the CO column density is 10^{18} cm^{-2} while C2 and CO excitation reveals a temperature of 10 K and density about 1000 cm^{-3}, more like conditions found in dark molecular clouds. Similar results arise from our chemical analysis for CN through reactions involving observations of CH, C2, and NH. Enhanced potassium depletion and a reduced CH/H2 column density ratio also suggest the presence of a dark cloud. The directions toward HD27778 and HD30122 probe molecule-rich diffuse clouds, which can be considered CO-dark gas, while the sight line toward HD28975 represents an intermediate case. Maps of dust temperature help refine the description of the material along the four sight lines and provide an estimate of the distance between HD29647 and a clump in the TMC. An Appendix provides results for the direction toward HD26571; this star also probes diffuse molecular gas.